Proceedings of the 2021 IEEE
International Conference on Robotics and Biomimetics
December 27-31, 2021, Sanya, China

2021 IEEE International Conference on Robotics and Biomimetics (ROBIO) | 978-1-6654-0535-5/21/$31.00 ©2021 IEEE | DOI: 10.1109/ROBIO54168.2021.9739351

Bio-inspired Soft (BIS) Hand for Tele-operated COVID-19 Oropharyngeal (OP) Swab Sampling

Jianshu Zhou†, *Member*, *IEEE*, Wei Chen†, Shing Shin Cheng, *Member*, *IEEE*, Lingbin Xue, Michael C. F. Tong and Yunhui Liu, *Fellow*, *IEEE*

***Abstract*—The lasting difficulty imposed by the COVID-19 pandemic has made profound challenges to our daily lives. The prominent task to contend with the COVID-19 is the diagnosis of the SARS-CoV-2 virus. The timely diagnosis guides further anti-infection measurements such as effective quarantine and dedicated therapy. Existing diagnosis majorly relies on manual face-to-face Oropharyngeal (OP) and Nasopharyngeal (NP) sampling, which results in high infection risk and heavy working burden to medical staff. Robotic sampling is a promising solution for this challenge because robots are intrinsically immune to viruses and working without fatigue. Following this target, we demonstrate our novel teleoperated OP swab sampling system with excellent safety guarantees, quick deployability, and task efficacy. A bio-inspired soft hand integrated with a soft wrist is developed, which can pick and manipulate the disposable swab as dexterous as a human hand. Stereo imaging is provided to the operator by a terminal binocular camera. The design, working mechanism, and control of our sampling system are discussed. Results show that our proposed robotic sampling system promises safe and effective OP swab sampling to protect medical staff and convenient the sampling process.**

***Index Terms*- COVOID-19 OP Sampling, Bio-inspired Soft Hand, Teleoperation System.**

I. INTRODUCTION

COVID-19 has profoundly affected our daily lives around two years since its original breakout [1-6]. Although massive effort around the world has been made to contain COVID-19, the pandemic remains active, and the case number is still rising. The SARS-CoV-2 virus has demonstrated high contagiousness and infection fatality rate and can be carried by quite a few asymptomatic carriers [2, 3]. Even in regions where local infection cases have been eliminated by burdensome means such as lockdown and community testing, they are still susceptible to the return of the infection cases due to the versatile transmission routes of the virus [4, 5]. The struggle between the epidemic and humans may continue for years until herd immunity is achieved.

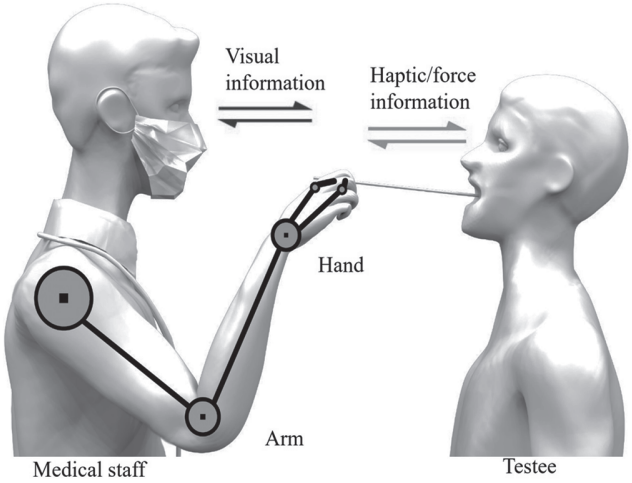


Figure 1. Illustration of human OP swab sampling for COVID-19 diagnosis.

The prominent task to counter COVID-19 is the initial diagnosis of the SARS-CoV-2 virus [2, 6]. Timely diagnosis guides further anti-infection measurements such as effective quarantine and dedicated therapy. Currently, most countries and WHO have recommended the nasopharyngeal (NP) and oropharyngeal (OP) swab sampling for COVID-19 specimen sampling and diagnosis [2, 7]. The existing realization of OP and NP swab sampling majorly relies on medical staff to swab patients face-to-face manually, as illustrated in Fig. 1. Face-to-face sampling in potential virus carriers requires a large number of quantified medical staff and unavoidably exposes the medical staff to potential infection danger. The doctors or nurses have to be armed with heavy protection suits from head to foot. This results in a heavy working burden and yet does not completely eliminate the risk of infection [2, 6].

Robotic sampling is a promising solution for this challenge because robots are intrinsically immune to viruses and can work without experiencing fatigue [1, 6]. The introduction of robots aims to improve the automation and efficiency of the COVID-19 swab sampling process [6-8]. With sampling force limited in the range from 10 to 60 g, a swab robot is developed with a preliminary test [9]. In terms of assisting human labor swab sampling, a low-cost miniature robot that can be deployed efficiently has been

This work was supported in part by National Key Research and Development Program of China under Grant 2018YFB1309300. The work was supported in part by Hong Kong RGC via the TRS project T42-409/18-R and 14202918, the Hong Kong Centre for Logistics Robotics, CUHK T Stone Robotics Institute, and in part by the CUHK Hong Kong-Shenzhen Innovation and Technology Research Institute (Futian).

†JS Zhou and W Chen are joint first authors.

JS Zhou, W Chen, SS Cheng, and YH Liu are with the T Stone Robotics Institute, the Department of Mechanical and Automation Engineering, The Chinese University of Hong Kong. JS Zhou and YH Liu are also with the Hong Kong Center for Logistics Robotics (HKCLR). (jianshuzhou@cuhk.edu.hk)

LB Xue and Michael C. F. Tong are with the Department of Otorhinolaryngology, Head and Neck Surgery, The Chinese University of Hong Kong.

© IEEE 2022. This article is free to access and download, along with rights for full text and data mining, re-use and analysis.

reported [10]. A swab sampling robot based on remote collaborative control has been presented [11]. Besides, collaborative robot arms have been applied to mount versatile end-effectors dedicated to swab sampling [12, 13].

However, the current sampling robot solution has two challenges. One is how to ensure the safety of testee when sampling by a bulky and rigid robot and operating inside the marrow oral cavity with delicate soft tissue; the second is how to replicate human operation dexterity in a compact size and lightweight robotic system. For example, in a real OP sampling process, testee sometimes will cough due to discomfort. This results in a potential human-robot collision with operational risk. Besides, successful sampling requires dexterous manipulation of the swab in a confined space. Considering safety, comfort, and dexterity, current robots are significantly inferior compared to human operations.

Recent advances in soft robotic technology demonstrate a solution for dexterous robotic hand design with intrinsic compliance for safe and effective grasping and manipulation [14-22]. These examples provide a promising potential for OP swab sampling with enhanced dexterity and intended safety.

In this work, we present a bio-inspired soft (BIS) hand dedicated to safe and dexterous OP swab sampling. The BIS hand is designed based on human hand sampling observation, which well replicates the pinch function of human fingers and orientation adjustment of the human wrist. Two fingers of BIS hand are integrated with a stereo camera and LED light source for oral visual information collection. Besides, a force sensor is embedded in the wrist for sampling force measurement. By mounting BIS hand at the terminal of a collaborative arm, the complete robotic system provides a human comparable dexterity for OP swab sampling. A teleoperation-based controller is applied with a Geomagic master device for human manipulators. Dedicated experiments are presented to validate the effectiveness of our proposed sampling system. The results show our proposed BIS hand-enabled robotic system provides a promising solution for teleoperated OP swab sampling.

II. Bio-inspired Soft (BIS) Hand and Tele-operated Sampling System Design

This section introduces the novel BIS hand design and its working mechanism inspired by human sampling observation. Besides, the whole sampling system is also illustrated.

A. Human Manual Sampling Observation

Before our robot design, we paid attention to the well-trained healthcare workers and studied the necessary factors for successful swab sampling. From the observation, there are three essential components [2, 6], as shown in Fig. 1. The first is the arm that allows the hand to approach the mouth of the testee. The second function is achieved by the wrist for swab orientation tuning. The third is the fingers (particularly the thumb, the index finger, and the middle finger) applied to pinch and operate the swab firmly. From the sensory perspective, there are two critical sensing components involved in the manual sampling process. They are visual feedback and tactile feedback.

Thus, our goal is to build a robot system that achieves these two perceptions and certain physical functions with a human manual sampling comparable performance.

B. Bio-inspired Soft (BIS) Hand Design

How to achieve human hand pinch function with dexterous reorientation capability in a confined structure is challenging. A novel bio-inspired soft (BIS) hand is proposed as depicted in Fig. 2(a). The BIS hand is majorly composed of two parts. One is the soft-rigid hybrid gripper, and the second is the continuum dexterous wrist. For sensory information collection, two fingers are embedded with a binocular camera and a led respectively for oral visual information detection. Besides, a force sensor is embedded in the wrist for sampling force measurement.

The soft-rigid hybrid gripper can achieve a human finger comparable pinch function as illustrated in Fig. 2(b1-b2) [15-18]. The surface of the gripper is designed by soft adaptable material for the adaptable grasping of generally used disposable swabs. The phalange of the gripper (label in Fig. 2) is rigid for grasping robustness. The joint of the gripper is a soft pneumatic actuator with excellent actuation and response efficiency, inherent compliance, and adjustable output force. The working mechanism of the soft-rigid hybrid gripper is depicted in Fig. 2(c). For each finger, a soft actuator is mounted within a pin joint. Positive pneumatic input will expand the soft actuator and close the fingers together; negative pneumatic input will shrink the soft actuator and open the fingers [15-18]. By adjusting the desired pneumatic input, the joint motion and pinch force can be well adjusted. The two phalanges of the gripper are designed in a hollow structure to embed a led (CRISPI-Q5) and a binocular camera (MSK-SM, 1/2.7 CMOS & 8500mmIR) inside.

The dexterous reorientation of the gripper is achieved by a continuum dexterous wrist as shown in Fig. 2(b3-b5). The dexterous wrist is designed in the form of a multi-backbone continuum structure with a diameter at 42 mm, as shown in Fig. 2(d). The inner backbone is a pneumatic backbone with pre-charged pneumatic input while the outer backbone provides the actuation and sensor channels. The soft wrist stiffness can be adjusted by using the pre-charged pneumatic input of the inner backbone [23]. Three driving cables are used to bend the universal wrist joint through differential actuation [24]. It is capable of bending 81° in any direction. A compact control box, containing 3 minimized servo motors (MG996R-15kg), is used to actuate the dexterous wrist.

A force sensor (DYZ-101) is mounted at the terminal of wrist. The sampling force of the soft gripper in the axial direction can be timely measured by the force sensor.

Besides, the BIS hand is fully waterproof to allow disinfection and untethered for easy deployment. The gripper and wrist are conveniently detachable for quick components replacement and update. All the soft components are fabricated through soft material molding and 3D printing technology [18-21]. Major design parameters of BIS hand are illustrated in Table. I.

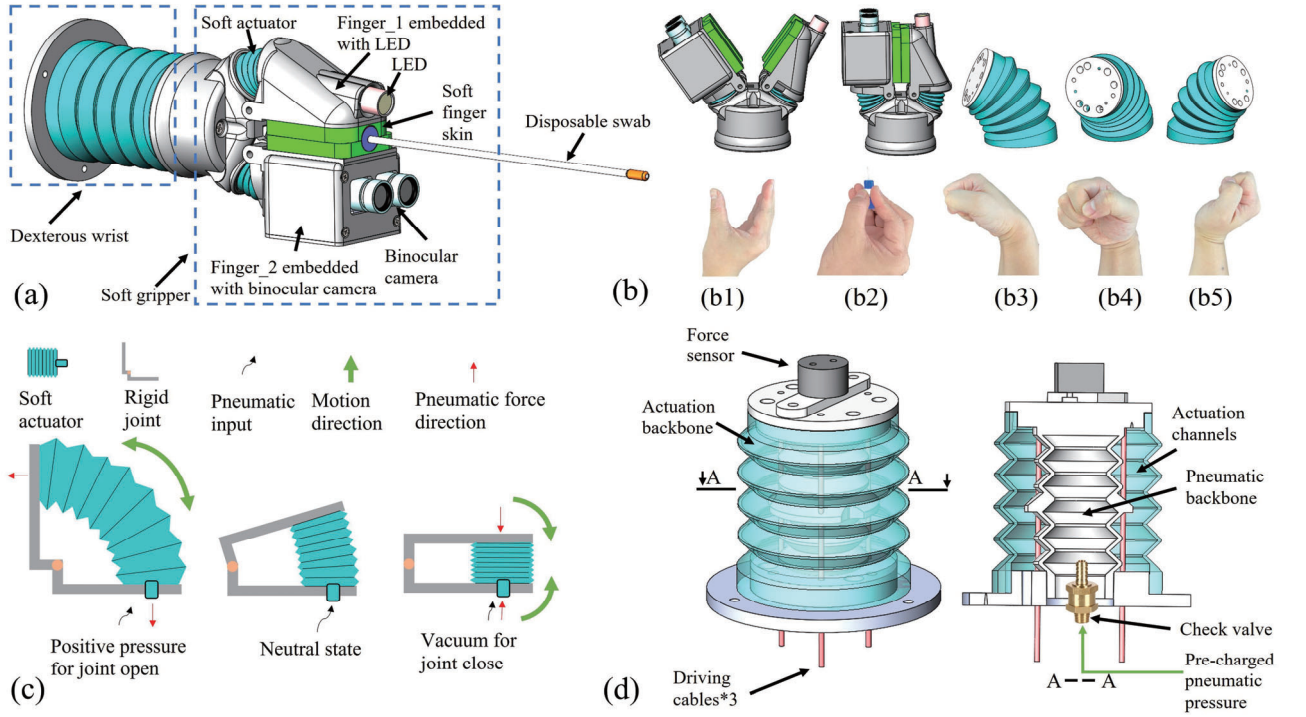


Figure 2. Bio-inspired soft (BIS) hand design and working mechanism. (a) The construction of BIS hand. (b) Swab picking and reorientation dexterity enabled by a dexterous gripper (b1-b2) and a soft wrist (b3-b5). (c) The working mechanism of soft-rigid hybrid joint for soft gripper. (d) The working mechanism of multi-backbone soft continuum robot for soft wrist, which leverages the pre-charged pneumatic input for stiffness adjustment.

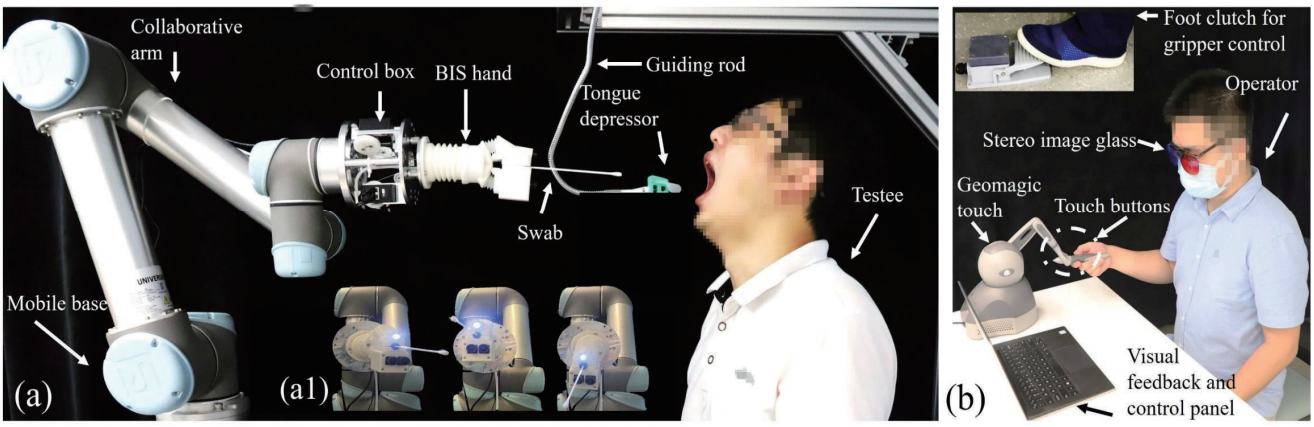


Figure 3. The illustration of overall teleoperated sampling system. (a) The slave sampling system on the testee part. (a1) Front view of BIS hand swab manipulation. (b) The master sampling system on the operator's part.

TABLE I. BIS HAND MAJOR DESIGN PARAMETERS

Feature	Parameter
Soft gripper material	3D printed PLA
Soft wrist material	3D printed TPU
Height of the gripper	80 mm
Length of the wrist	55 mm
Diameter of the wrist	42 mm
Weight of the hand	160 g
Weight of the control box	260 g
Waterproof	Yes

C. Teleoperated OP Swab Sampling System Design

The overall sampling system is illustrated in Fig. 3, where Fig. 3(a) presents the slave system of the sampling robot interacting with the testee, and Fig. 3(b) illustrates the master system handled by the operator [25]. The master and slave systems can be placed remotely in two separate rooms or regions.

In the slave system, a guiding rod with a disposable tongue depressor at its terminal is leveraged to provide a reference location for the robot to insert the swab into the oral cavity. The testee would be asked to bite the tongue depressor before the operator makes fine position and orientation adjustment of the collaborative robot arm through a dedicated control user interface (UI) on the master side. Then, the operator can teleoperate the system to insert the swab into mouth cavity and manipulate the BIS hand for dexterous sampling.

On the master side, the operator can control the pinch

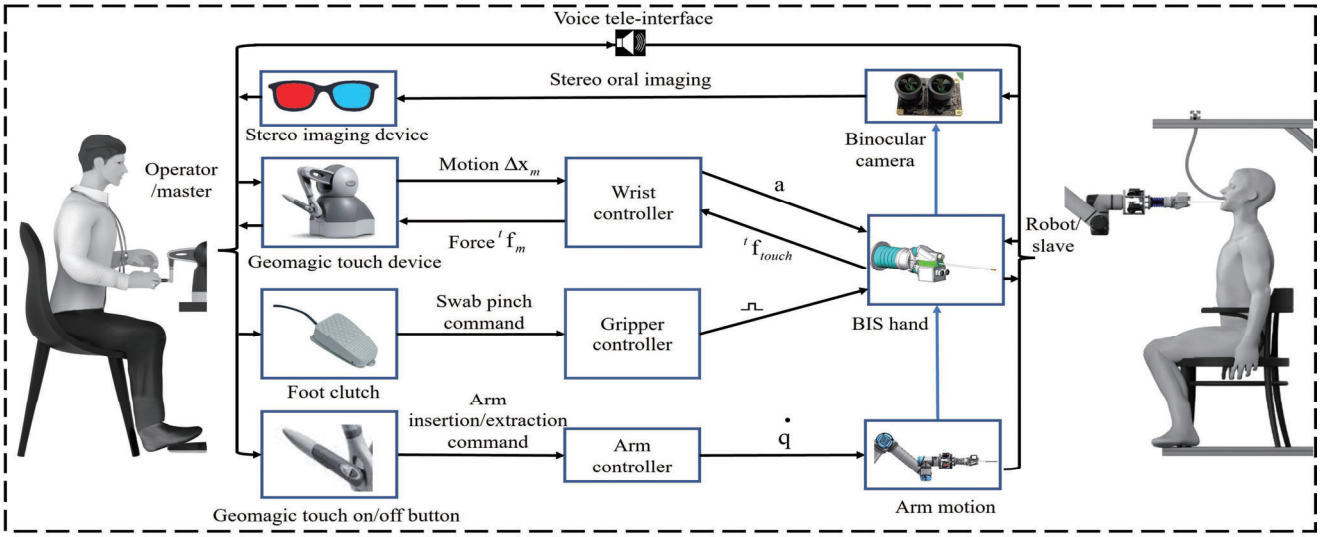


Figure 4. Teleoperation framework illustration for teleoperated OP swab sampling system.

function of the gripper through a foot clutch. The BIS hand orientation is adjusted by Geomagic touch, while the insertion and extraction of the arm are controlled by two touch buttons on the Geomagic touch manipulator.

To provide intuitive visual feedback with depth information, a stereo image generation system is utilized. The operator wearing 3D glasses can observe the stereo oral cavity visual feedback, which will be discussed in detail in Section IV B.

III. Teleoperation Based on Visual and Force Cues

This section introduces our teleoperation framework based on visual and haptic cues for OP swab sampling. Force virtual fixture for OP swab sampling safety guarantee is also discussed.

A. Teleoperation Framework and Its Realization

The overall teleoperation controller is constructed by three sub-controllers, the soft gripper controller, the soft wrist controller, and the robot arm controller.

For the soft gripper controller, we applied a simple on/off control with the pre-calibrated grasping force for versatile swabs. In this work, we applied 60 kPa pneumatic input for swab pinch. The signal is generated by a foot clutch trodden by the operator. Treading the clutch provides the pinch command to the gripper and releasing the clutch provides the releasing command to the gripper.

For the soft wrist controller, a point-to-point motion controller is applied from the Geomatic touch to the soft wrist. The master motion is obtained by Geomagic touch manipulated by the operator. A point-to-point mapping is applied as:

$$\Delta x_S = \frac{1}{k_{motion}} {}^{S} J_m \Delta x_m \tag{1}$$

where the human hand motion $\Delta x_m \in R^3$ is converted to the robot motion $\Delta x_S \in R^3$ by the motion scaling factor k_{motion}. With the help of this scale adjustment, the swab movement can be limited in the narrow throat space. For example, when the motion scale factor $k_{motion} = 2$, the converted motion target Δx_S is half of the operator's motion Δx_m. ${}^{S} J_m$ is the motion coordinate transformation matrix, which maps the motion between the master frame and the slave frame and pre-calibrated as:

$$s_{J_m} = \begin{bmatrix} 0 & -1 & 0 \\ -1 & 0 & 0 \\ 0 & 0 & -1 \end{bmatrix} \tag{2}$$

In terms of the arm controller, as the guiding rod has already provided a reference position for the oral cavity of the testee, the major duty of the arm is the insertion and extraction of the BIS hand to the desired position. The insertion and extraction command is provided by the touch buttons on the Geomagic handle. If the operator finds the oral cavity of testee is not in the center of BIS hand, spatial position and orientation adjustment of the arm can be achieved by our dedicated operation user interface.

B. Force Virtual Fixture (VF) for Sampling Safety

To ensure the testee's safety during the sampling process, a force-based virtual fixture (VF) is applied [26]. In real sampling, due to the flexibility of the disposable swab, the axial sampling force is remarkably larger than the lateral sampling force. Constraining the axial sampling force in the desired range provides a safe and relatively comfortable sampling.

As introduced in Section II.B, a one-dimensional minimized force sensor is embedded in the dexterous wrist. f_l is denoted as the axial force measured in real-time. When f_l exceeds the preset threshold $f_{threshold}$, the controller will shorten the length of soft wrist by using the admittance control:

$$\dot{l} = k_{stiffness}(f_{threshold} - f_l), \tag{3}$$

where $k_{stiffness}$ is admittance gain. The specific shorten length was off-line calibrated to compensate the

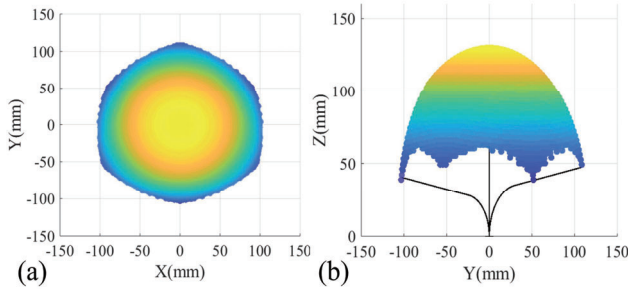


Figure 5. Workspace of BIS hand. (a) Top view. (b) Lateral view.

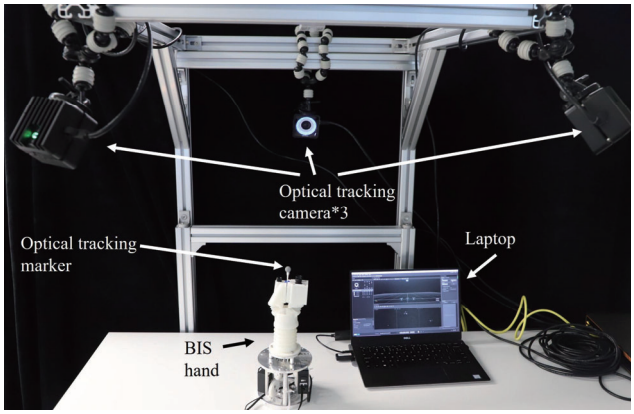


Figure 6. Experimental setup for BIS hand trajectory tracking performance evaluation.

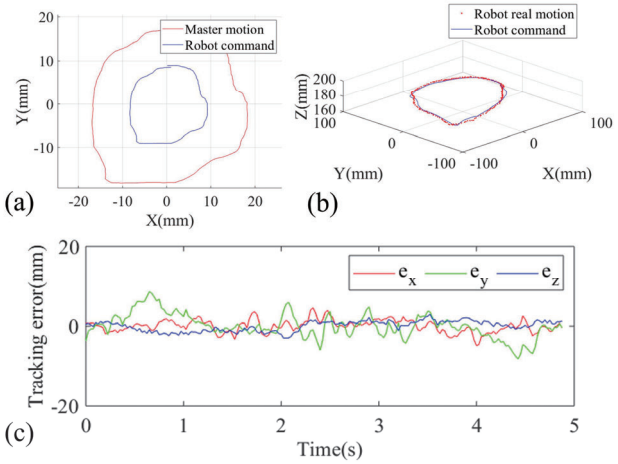


Figure 7. Teleoperated trajectory tracking performance. (a) Master motion and robot command trajectory. (b) The robot command and captured robot trajectory. (c) Trajectory tracking error.

force increment. Constrained by the force virtual fixture, f_l can be guaranteed in a safe range.

The force feedback is directly calculated by transfer axial sampling force f_l to the task space:

$$f_s = \mathrm{J}[0 \quad 0 \quad f_l]^T, \tag{4}$$

where J is the Jacobian matrix of BIS hand mapping the motion between the configuration space and the task space. Finally, the force is transferred to the Geomagic touch by the force feedback scale variable k_{force}:

$$f_m = k_{force}\,{}^m\mathrm{J}_s f_s, \tag{5}$$

where ${}^m\mathrm{J}_s$ is the inverse matrix of ${}^s\mathrm{J}_m$.

IV. Experimental Validation

To evaluate the performance of the proposed OP swab sampling system and BIS hand, several experiments were carried out. Firstly, we evaluated the workspace of the BIS hand. Then, the trajectory tracking performance of the BIS hand is measured. Thirdly, the realization of stereo image visual feedback is presented. After that, the overall sampling success rate and sampling force were evaluated followed by the human user demonstration.

A. BIS Hand Workspace and Trajectory Tracking

The achievable workspace of BIS hand is important for sampling dexterity. The workspace of BIS hand was simulated as shown in Fig. 5. The BIS hand has a similar and comparable workspace compared to that of operations by human, which guarantees dexterous swab sampling [29]. The ability of the BIS hand to adjust its wrist length depending on the desired stiffness further provides functionality augmentation in terms of the workspace and stiffness variation, compared to the human hand.

Trajectory tracking performance of the robot is important for effective teleoperation. We processed a trajectory tracking evaluation test on the BIS hand as depicted in Fig. 6 [30, 31]. Three optical tracking cameras were hung over the BIS hand, which pinched a tracking marker. Dedicated trajectories were generated and used as the reference command for the BIS hand. Real hand tracking trajectory was captured by the optical tracking camera. Results are shown in Fig. 7(a) and Fig. 7(b) demonstrate the rectangular and circular trajectories tracking performance respectively. The three-dimensional tracking error in Fig. 7(a) and Fig. 7(b) are depicted in Fig. 7(c). The BIS hand was able to track the human hand's motion smoothly with a control frequency at 25 Hz. The root-mean-square tracking error was (1.5428, 3.0128, 1.2398) mm in X, Y, and Z axes respectively, which is an acceptable performance for teleoperation on a soft hand with inherent compliance.

B. Stereo-image Feedback Generation

As introduced in Section II C, to provide the doctors/nurses with an intuitive feeling, we used an anaglyph approach to generate 3D vision for visual feedback [27, 28]. The left image I_{left} and right image I_{right} were collected from the stereo camera. Secondly, the filters (red and blue or cyan) were applied to these two images, which were then combined to generate the anaglyph image $I_{anaglyph}$. The formulation can be expressed as:

$$I_{anaglyph} = \Gamma_{left} I_{left} + \Gamma_{right} I_{right}, \tag{6}$$

where Γ_{left} and Γ_{right} are the two filter matrices. The anaglyph image, $I_{anaglyph}$, seen through the anaglyph glasses, provides the depth perception, which can help doctors operate more accurately.

C. Teleoperated Sampling Success Rate and Safety Evaluation

To evaluate the sampling success rate, our teleoperated

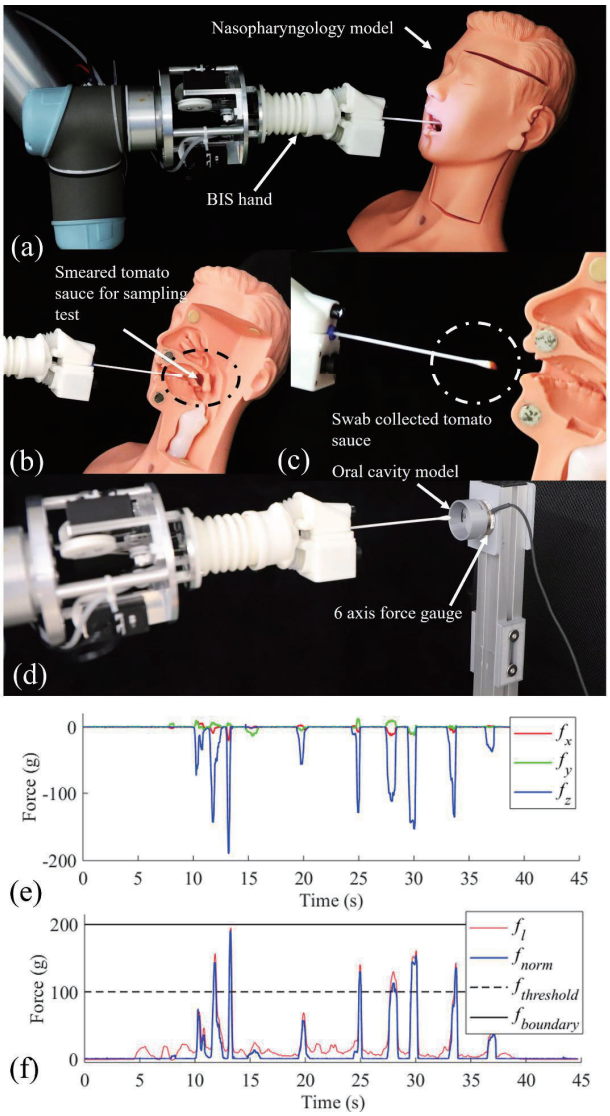


Figure 8. Teleoperated OP sampling success rate and sampling force safety evaluation. (a) Success rate of sampling test on an oral model. (b) Tomato sauce smeared on the throat for swab collection. (c) Swab collected tomato source. (d) Platform for sampling force collection. (e) Sampling force information measured from testing platform. (f) Calculated norm force for force virtual fixture restriction.

sampling robot has experimented on an oral phantom model. The experiment setup is shown in Fig. 8(a) where an oral phantom model was put on the table facing the sampling robot. The tomato source was smeared on the throat surface as illustrated in Fig. 8(b), which was regarded as the potential virus attached to the surface of oral tissue. For the stiffness setup, the wrist stiffness was set to the maximum level with 90 kPa input pressure [19, 21, 32].

A successful sampling case was considered when the swab surface contains the tomato source, as depicted in Fig. 8(c). Twenty sampling tests were performed and all these cases were successful.

To test the real-time sampling force and the effectiveness of the force VF constraint, a sampling force experiment was performed on a circular ring-sized oral cavity model of 40mm diameter as shown in Fig. 8(d). An ATI Nano-43 (ATI Industrial Automation) force sensor, was installed in the model to record the sampling force in the task space. A period of measured data is shown in Fig. 8(e). The boundary of the sampling threshold is set to be 100 g, as displayed in Fig. 8(f), which ensures a 200 g sampling boundary with the dedicated VF controller introduced in Section III.B. When the measured axial sampling force, f_l, exceeded the threshold, the controller would shrink the wrist length and generate high operation resistance for Geomagic touch to inform the operator. f_{norm} was the real-time calculated square root value of the quadratic sum of f_x, f_y, and f_z. f_{norm} was also restricted within the $f_{boundary}$, which proved the efficacy of the VF constraint of our sampling system and the sampling force can always be constrained within the desired threshold.

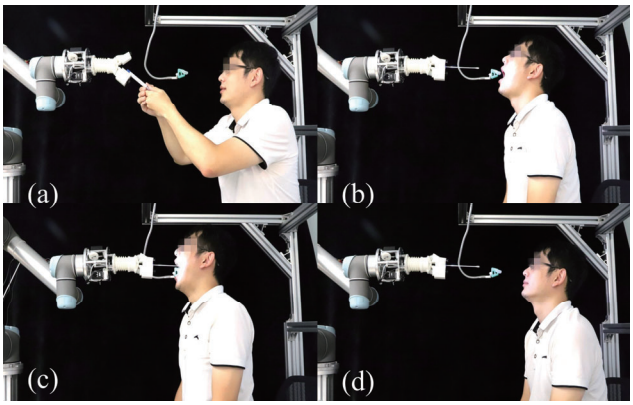


Figure 9. Demonstration of teleoperated OP swab sampling for human user.

The results proved that the high sampling success rate can be achieved by the dexterous BIS hand and sampling safety can be ensured by the BIS hand compliance accompanied with the force virtual fixture.

D. Human User Demonstration

After the sampling performance verification, we present a user demonstration to illustrate a general sampling pipeline. The system configuration is illustrated in Fig. 3, in which a testee was seated facing to the sampling robot. The entire sampling process is illustrated in Figs. 9(a)-9(d) and described as follows:

Oropharyngeal sampling procedure:

Step_i Sampling preparation and swab replacement: The testee sit facing the sampling robot and the sampling robot is turned on by the operator as illustrated in Fig. 9(a). The testee assisted the robot to pick a new swab for sampling and replace a tongue depressor to bite.

Step_ii Sampling preparation and testee bites the tongue depressor: The testee opens the mouth in front of the TSS hand waiting for sampling as illustrated in Fig. 9(b). The operator informs the testee to bite the tongue depressor to prepare for testing.

Step_iii Swab insertion and sampling: After the testee firmly bit the tongue depressor, the operator moved the robot arm to insert the swab into the oral cavity of the testee and manipulated the wrist to perform teleoperated swab sampling as presented in Fig. 9(c).

Step_iv Swab extraction and storage: After sampling, the robot removed the swab as shown in Fig. 9(d) and the testee assisted the sampling robot to remove and store the swab.

V. Conclusion and Future Work

In this work, we demonstrate a novel bio-inspired soft (BIS) hand for safe and effective OP swab sampling. By observing medical staff sampling, two sensing modalities (i.e., visual and tactile feedback), and three interaction parts (i.e., arm, wrist, and hand) are critical. We achieved these functions by our soft robot hand mounted on a collaborative arm integrated with a force sensor and binocular camera. The robotics sampling system intends to achieve a human sampling comparable dexterity and maneuverability. Force virtual fixture is applied to give a safety sampling procedure. We carried out comprehensive experiments, which include BIS hand workspace, the teleoperated trajectory tracking accuracy, and safety of teleoperated OP sampling, to validate the proposed robotic sampling system. Results show a prominent sampling success rate enabled by the BIS hand dexterity. The experimental results prove the merits of our proposed soft robotics enabled OP sampling system ensuring both sampling dexterity and safety.

In the future, we will seek ethical approvals for our OP sampling system to perform the in-vivo test, further improve the BIS hand, involve AI-based controller to provide a fully automatic sampling procedure, and transfer the sampling system to two collaborative arms with two BIS hands to get rid of human assistance for swab replacement and storage.

REFERENCES

[1] Yang G Z, Nelson B J, Murphy R R, et al. Combating COVID-19—The role of robotics in managing public health and infectious diseases. 2020.

[2] https://www.who.int/zh/director-general/speeches/detail/who director-general-s-opening-remarks-at-the-media-briefing-on-covid-19-5-march-2021

[3] Centers for Disease Control and Prevention, Interim Guidelines for Collecting, Handling, and Testing Clinical Specimens from Persons Under Investigation (PUIs) for Coronavirus Disease 2019 (COVID-19), 9 March 2020; www.cdc.gov/coronavirus/2019-ncov/lab/guidelinesclinical-specimens.html.

[4] Bandyopadhyay, S., Baticulon, R. E., Kadhum, M., Alser, M., Ojuka, D. K., Badereddin, Y., ... & Khundkar, R. (2020). Infection and mortality of healthcare workers worldwide from COVID-19: a scoping review. medRxiv.

[5] Sanche, S., Lin, Y. T., Xu, C., Romero-Severson, E., Hengartner, N., & Ke, R. High contagiousness and rapid spread of severe acute respiratory syndrome coronavirus 2. Emerging infectious diseases, 2020, 26(7), 1470-147.

[6] Shen Y, Guo D, Long F, et al. Robots under COVID-19 Pandemic: A Comprehensive Survey. IEEE Access, 2020.

[7] Yang, G., Lv, H., Zhang, Z., Yang, L., Deng, J., You, S., ... & Yang, H. (2020). Keep healthcare workers safe: application of teleoperated robot in isolation ward for COVID-19 prevention and control. *Chinese Journal of Mechanical Engineering*, 33(1), 1-4.

[8] Petruzzi G, De Virgilio A, Pichi B, et al. COVID - 19: Nasal and oropharyngeal swab. *Head & neck*, 2020, 42(6): 1303-1304.

[9] Li, S. Q., Guo, W. L., Liu, H., Wang, T., Zhou, Y. Y., Yu, T., ... & Li, S. Y. (2020). Clinical application of an intelligent oropharyngeal swab robot: implication for the COVID-19 pandemic. European Respiratory Journal, 56(2).

[10] Wang S, Wang K, Tang R, et al. Design of a low-cost miniature robot to assist the COVID-19 nasopharyngeal swab sampling. *IEEE Transactions on Medical Robotics and Bionics*, 2020.

[11] Ying-Long, C., Fu-Jun, S., & Yong-Jun, G.. Remote Human-robot Collaborative Impedance Control Strategy of Pharyngeal Swab Sampling Robot. In 2020 5th International Conference on Automation, Control and Robotics Engineering (CACRE) (pp. 341-345). IEEE.

[12] Robot swabs patients' throats for Covid-19. Accessed: Mar. 25, 2021. [Online].Available:https://www.sdu.dk/en/nyheder/forskningsnyheder/robot-kan-pode-patienter-for-covid-19.

[13] Robots That Can Water Your Plants and Swab Your Throat. Accessed: Mar. 25, 2021. [Online]. Available: https://www.caixinglobal.com/2020-09-07/gallery-robots-that-can-water-your-plants-and-swab-your-throat-101602237.html

[14] Rus D, Tolley M T. Design, fabrication and control of soft robots. Nature, 2015, 521(7553): 467-475.

[15] Zhou, J., Chen, S., & Wang, Z. (2017). A soft-robotic gripper with enhanced object adaptation and grasping reliability. *IEEE Robotics and automation letters*, 2(4), 2287-2293.

[16] Zhou J, Yi J, Chen X, et al. BCL-13: A 13-DOF soft robotic hand for dexterous grasping and in-hand manipulation. *IEEE Robotics and Automation Letters*, 2018, 3(4): 3379-3386.

[17] Zhou J, Chen X, Chang U, et al. A soft-robotic approach to anthropomorphic robotic hand dexterity. *Ieee Access*, 2019, 7: 101483-101495.

[18] Zhou, J., Chen, X., Li, J., Tian, Y., & Wang, Z. (2018, April). A soft robotic approach to robust and dexterous grasping. In 2018 IEEE International Conference on Soft Robotics (RoboSoft) (pp. 412-417). IEEE.

[19] Zhou J, Chen Y, Hu Y, et al. Adaptive Variable Stiffness Particle Phalange for Robust and Durable Robotic Grasping. *Soft robotics*, 2020, 7(6): 743-757.

[20] Zhou J, Chen X J, Chang U, et al. Intuitive control of humanoid soft-robotic hand BCL-13. 2018 IEEE-RAS 18th International Conference on Humanoid Robots (Humanoids). IEEE, 2018: 314-319.

[21] Zhou J, Chen Y, Chen X, et al. A proprioceptive bellows (PB) actuator with position feedback and force estimation. *IEEE Robotics and Automation Letters, 2020*, 5(2): 1867-1874.

[22] Chen, W., Zhou, J., Cheng, S. S., Lu, Y., Zhong, F., Gao, Y., ... & Liu, Y. H. Tele-Operated Oropharyngeal Swab (TOOS) RobotEnabled by TSS Soft Hand for Safe and EffectiveCOVID-19 OP Sampling. arXiv preprint arXiv:2109.09403.

[23] Li Y, Chen Y, Ren T, et al. Precharged pneumatic soft actuators and their applications to untethered soft robots. *Soft robotics*, 2018, 5(5): 567-575.

[24] Jones B A, Walker I D. Kinematics for multisection continuum robots. *IEEE Transactions on Robotics*, 2006, 22(1): 43-55.

[25] Okamura A M. Methods for haptic feedback in teleoperated robot-assisted surgery. *Industrial Robot: An International Journal*, 2004.

[26] Abbott J J, Okamura A M. Pseudo-admittance bilateral telemanipulation with guidance virtual fixtures. *The International Journal of Robotics Research*, 2007, 26(8): 865-884.

[27] Livatino S, Muscato G. Robot 3D vision in teleoperation. World Automation Congress 2012. IEEE, 2012: 1-6.

[28] Livatino S, De Paolis L T, D'Agostino M, et al. Stereoscopic visualization and 3-D technologies in medical endoscopic teleoperation. *IEEE Transactions on Industrial Electronics*, 2014, 62(1): 525-535.

[29] Marshall M M, Mozrall J R, Shealy J E. The effects of complex wrist and forearm posture on wrist range of motion. *Human Factors*, 1999, 41(2): 205-213.

[30] Zhou, J., Chen, X., Chang, U., Liu, Y., Chen, Y., & Wang, Z.. A grasping component mapping approach for soft robotic end-effector control. In 2019 2nd IEEE International Conference on Soft Robotics (RoboSoft) (pp. 650-655). IEEE.

[31] Zhou, J., Li, Y., Yang, Y., Cao, H., Huang, J., & Liu, Y. (2021, July). A 22-DOFs Bio-inspired Soft Hand Achieving 6 Kinds of In-hand Manipulation. In 2021 IEEE International Conference on Real-time Computing and Robotics (RCAR) (pp. 20-26). IEEE.

[32] Li, D. C. F., Wang, Z., Zhou, J., & Liu, Y. H. Honeycomb Jamming: An Enabling Technology of Variable Stiffness Reconfiguration. *Soft Robotics*. 2021.